3J2-1

Directivity of the Photoacoustic Signal Radiated from a Liquid-Filled Thin Elastic Tube

Wang Kun†, Yuji Wada, and Kentaro Nakamura
(Institute of Innovative Research, Tokyo Tech)

1. Introduction

Angiography for small blood vessels through the photoacoustic effect caused by the absorption due to hemoglobin has been intensively studied [1]. The authors, on the other hand, have investigated a method for evaluating contrast agents for photoacoustic imaging. The sample liquid is prepared in a thin tube less than 1 mm in diameter embedded in a phantom, and the photoacoustic signal is measured by irradiating a pulsed light using a semiconductor laser [2]. It has become clear that acoustic resonance in the thin tube affects the photoacoustic signal. In this paper, we report numerical and experimental studies of the influence of physical properties such as tube hardness on the directivity of the photoacoustic signal.

2. Experimental setup

A capillary filled with black ink was embedded in a cube phantom (EXSEAL, H00-600J) 30 mm long, 28 mm high, and 28 mm wide. Light emitted from a pulsed semiconductor laser (LD: THORLABS, L637G1, wavelength, 637 nm; power, 1300 mW) was focused using a 4-mm diameter ball-lens onto the capillary. To receive the photoacoustic signal, a planar transducer of 5-MHz in the center frequency and 8 mm in diameter (JAPAN PROBE, 5K5I) was pressed against the side wall of the phantom. The output signal was amplified by 40 dB and observed with an oscilloscope.

As shown in **Fig. 1**, the transducers were placed around the sample tube at 45-degree intervals from the optical axis of the laser beam and received at seven different angles. A glass capillary with an outer diameter of 1.0 mm and an inner diameter of 0.75 mm and a silicon tube with an outer diameter of 1.0 mm and the inner diameter of 0.50 mm was used as sample tubes.

Examples of the temporal waveforms of the photoacoustic signal from the sample are shown in **Fig. 2** (laser pulse width: 230 ns). The signal was accompanied by ringing in the glass capillary, whereas there was almost no ringing in the silicon tube. In the glass capillary, it is considered that acoustic resonance modes are excited in the tube. The resonance frequencies are around 1.5 MHz for mode (1,0) and around 2.4 MHz for mode (2,0), respectively.

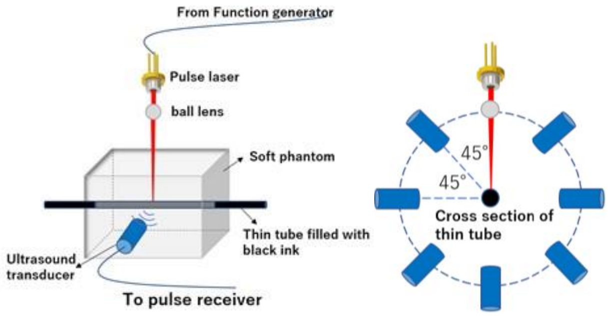

Fig. 1 Experimental setup for measuring the angular directivity of photoacoustic radiation.

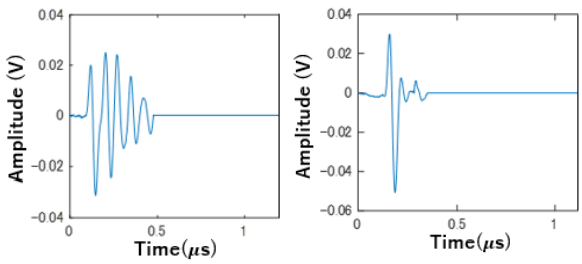

Fig. 2 Typical photoacoustic signals: left, a glass capillary (1.0 mm and 0.75 mm in outer and inner diameters); right, a silicone tube (1.0 mm and 0.5 mm in outer and inner diameters). The pulse width of the exciting light was 230 ns.

3. Simulation of directivity

Assuming a thin tube of 0.75 mm in diameter and 15 mm in length, the cross-section was divided into 72, 10, and 50 sections in the angular, radial, and longitudinal directions, respectively. A harmonic point source at the frequency f was placed at each center of the section. The amplitudes of the point sources were weighed in the shape of the acoustic resonance mode in the tube (a rigid-wall boundary was assumed), where J_m is the m-th order Bessel function. Observation points were located on the cross-sectional plane of the tube at a distance of 10 times the radius of the tube. Sound pressure at each observation point was obtained by summing all the contributions from the point sources, considering the distance d and the element volume ΔV. Therefore,

$$p \propto \sum \frac{e^{jkd}}{d} J_m(kr) \cos m\theta \, \Delta V.$$

Calculated and measured directivity characteristics at the frequencies for mode (1,0) and mode (2,0) are shown in **Fig. 3**. Each of the directivity patterns corresponds to the mode shape, and mostly agrees with the experimental results. On the other hand, in the case of the silicon tube, finite element method (FEM) analysis considering the mechanical properties of the tube wall was carried out at approximately 1.5 MHz. As shown in **Fig. 4**, almost no directivity was observed in the case of silicone tube This is because the reflection coefficient of the tube wall is low and acoustic modes are unlikely to occur inside the tube.

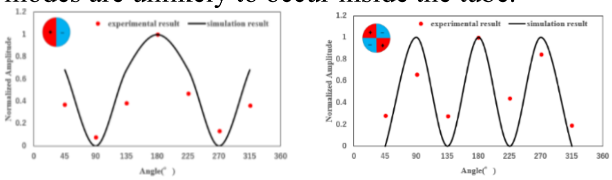

(1,0) resonance mode. (2,0) resonance mode.

Fig. 3 Directivity of photoacoustic signal in the case of a glass capillary.

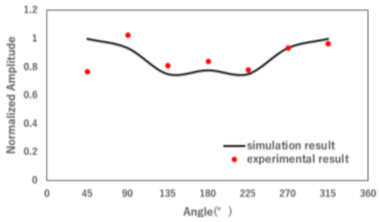

Fig. 4 Directivity of photoacoustic signal in the case of a silicone tube.

4. Frequency response of photoacoustic signals

Temporal waveforms of the ultrasonic signals emitted in the directions of 45°, 90°, and 180°, were calculated through FEM assuming a pulsed expansion source. the frequency responses were calculated and compared with experimental results. As demonstrated in **Fig. 5**, the glass capillary exhibits clear resonance, and the directivity depended on the mode shape in the same way in the experimental data. On the other hand, the silicon tube shows a broad characteristic compared to the glass capillary as shown in **Fig. 6**. High levels of DC or low-frequency components are probably because of the mono-polarity expansion source.

5. Conclusions

Directional characteristics of the emission of photoacoustic signals were investigated by irradiating the black-ink sample confined in a thin tube embedded in a phantom with a light pulse at 637 nm of wavelength. In the glass capillary, the acoustic resonance mode in the tube was intensively excited. On the other hand, no clear resonance was observed in the silicon tube because the acoustic impedance was close to that of the tube and the surrounding media, which resulted in weak confinement of acoustic waves. The directional characteristics of the photoacoustic signals varied accordingly.

In the future, we will try to estimate the stiffness of thin tubes from the photoacoustic responses.

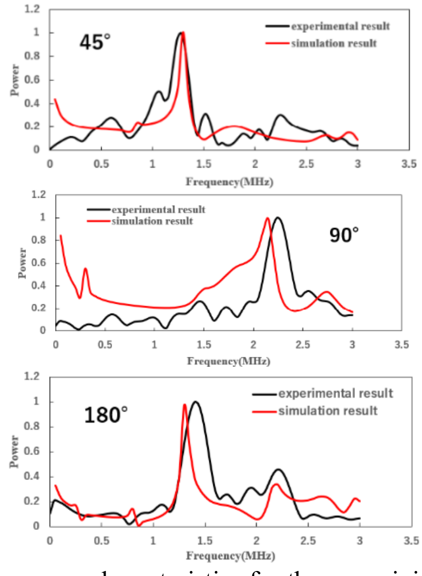

Fig.5 Frequency characteristics for three receiving angles for a glass capillary.

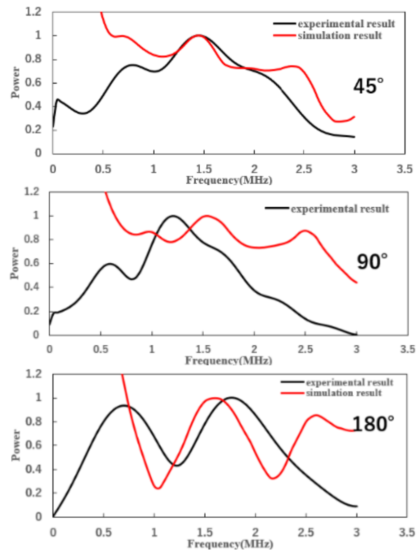

Fig.6 Frequency characteristics for three receiving angles for a silicon tube.

Acknowledgment

This work was supported by Grant-in-Aid for Scientific Research 18H01449.

References

1. S. Qu and K. Nakamura, IEICE Electronics Express, Vol.19, No.3, 1–6
2. S. Qu and K. Nakamura, AIP Advances, 11, 6, 065103, June 2021.
3. S. Qu and K. Nakamura, Engineering Research Express, 3, 045057, Dec. 2021.
4. M. Zhang et al., Elsevier Photoacoustics22, 2021
5. X. Zeng et al., Acoust. Sci. & Tech. 39 259, 2018.
6. T. Akimori et al., J. Laser Appl. 32 022070, 2020.